Anchor Self-Localization Algorithm for Ultrawideband Indoor Positioning System

Nikita Petukhov, Alexander Chugunov, Roman Kulikov, Natalya Masalkova, Tatiana Brovko

NRU MPEI
Moscow, Russia
nekitpetuhov@yandex.ru, iamchugunov@gmail.com, coolicoff@gmail.com, natasha.masalckova@yandex.ru, taanbrovko@gmail.com

***Abstract*—For infrastructure systems of indoor positioning, the issue of automating the calculation of anchor coordinates is relevant. This article presents a synthesized algorithm for self-localization of anchor coordinates for indoor positioning systems (IPS) based on ultra-wideband signals. The developed algorithm showed high accuracy (less than a millimeter) at the stage of simulation modeling.**

I. Introduction

Today, against the background of general technical progress, the relevance of tracking the movements of workers and positioning of various mobile platforms, such as, for example, automatically guided vehicles, is increasing. Global navigation satellite systems (GNSS) [1] are well-established standard for positioning, navigation and timing support. However, due to the fact that most part of production processes take place indoors, where GNSS signals are not available, there is a need for alternative systems that can provide positioning in such conditions. These systems are usually called indoor positioning systems (IPS).

At the moment, all known IPS can be divided by the type of technologies, on which they are built, into the following groups: optical systems [2], ultrasonic systems [3], inertial systems [4], odometric systems [5], magnetometric systems [6] and radio systems [7]. The advantages and disadvantages of each of the above systems are discussed in detail in [8] and are omitted from the narration in this article.

Radio systems seem to be the most suitable and equivalent in properties replacement for GNSS. Known IPS options based on the following radio standards are Wi-Fi, Bluetooth / Bluetooth low energy (BLE), ZigBee, Radiofrequency identification (RFID), NFER (Near-Field Electromagnetic Ranging), Ultra-WideBand (UWB). Of all the radio systems, it is worth highlighting the ultra-wideband radio systems, since they have the highest potential accuracy among all the above standards.

The UWB signal is a sequence of short pulses, due to which it is possible to effectively deal with the multipath problem that is urgent for the IPS. It consists in the fact that pulses corresponding to the direct signal path can be overlapped with pulses re-reflected from walls and various obstacles. In systems based on UWB signals, the probability of such an overlap is minimized (see Fig. 1) and their range resolution is sufficiently high, due to which their positioning error less than 10 cm and they are most attractive for a number of practical problems.

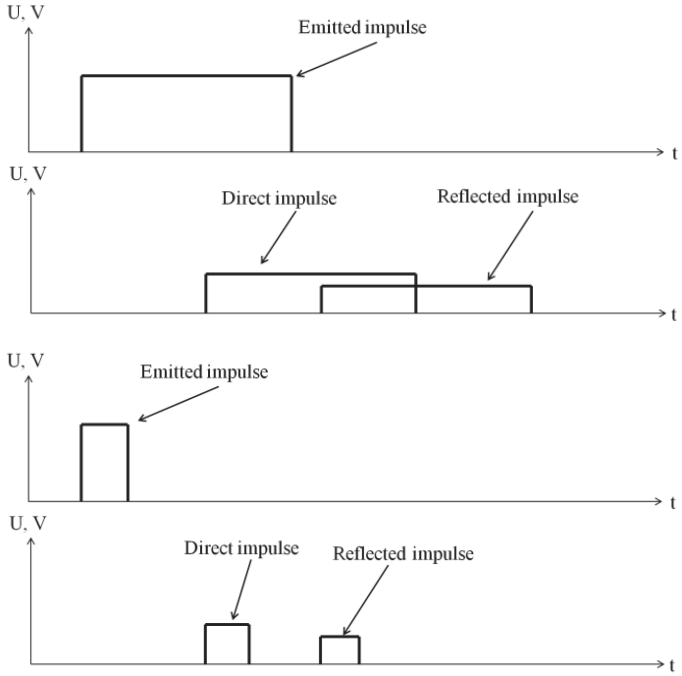

Fig.1. Advantage of ultrawideband signal over narrowband signal

Positioning in UWB-based IPS is implemented by intersection navigation methods. Intersection methods can be implemented in systems with different architectures, in which the measured parameters are: Time of Flight (ToF), Time of Arrival (ToA), Time Difference of Arrival (TDoA), Angle of Arrival (AoA), etc. All positional navigation methods are based on determining the unknown user location by one (or several) measured parameters, carried out by receiving a signal from radio navigation reference points (frequently called anchors) with previously known coordinates.

In most applications, the anchor points are set to a static position. Now the task of placing them in places with known coordinates during the deployment of the system is solved by careful initial alignment and calibration, performed manually by the operator or installer using expensive devices such as a

laser level and rangefinder. In addition to the fact that this process takes a lot of human effort and time, there are a number of practical applications with conditions dangerous to human life. Thus, it seems highly relevant to synthesize an algorithm for automatic determination of their positions by reference beacons using only radio measurements.

II. Problem statement

Given two anchors, placed in positions with known coordinates and a set of multiple measurements of relative distances between all the deployed anchors, taking into account their mutual radio visibility. Since the anchors are set in static positions, the measured relative distance between i-th and j-th anchor is represented in following form:

$$\breve{R}_{ij_k} = R_{ij_k} + n_k + \theta_k \cdot \delta \qquad (1)$$

where R_{ij_k} - true relative distance between i-th and j-th anchor, each sample from set is a discrete additive white Gaussian noise (AWGN) with zero mean and standard deviation σ_n, θ_k - function which equals 1 if abnormal NLOS error appears in measurement and equal 0 otherwise, δ - magnitude of abnormal NLOS error.

The main task is to estimate all the anchors coordinates with Kalman filter algorithm, processing measurements of relative distances between all the deployed anchors measurements taking into account their mutual radio visibility.

III. Algorithm

The first phase of algorithm consists in obtaining a sample of N_{init} measurements from each anchor. The measurements from each anchor are sorted into two groups: one of them includes the readings, the absolute difference of which with the previous readings has exceeded the specified threshold and the rest group contains the remaining ones. We leave the largest group, since it is assumed that NLOS abnormal errors are outliers, which appears in sample more rarely than normal measurements.

Further, the statistical characteristics of chosen part of measurements are estimated – mean and standard deviation, as well as the number of measurements in it. Important part of this phase of algorithm is compiling a matrix of anchor mutual radio visibility RV. This is a symmetric square matrix, the size of which is equal to the number of deployed anchors and consisting only of 0 and 1: if the i-th anchor received more than $N_{init}/3$ measurements from the j-th anchor, then element rv_{ij} is written equal to 1, otherwise it is considered that the there is no reliable radio path between anchors and the element is equal to 0.

For greater clarity, RV matrix for anchors radio visibility case in Fig.2 is shown below:

$$RV = \begin{bmatrix}
0&0&1&1&1&0&0&0&0&0&0&0&0&0&0\\
0&0&1&1&1&0&0&0&0&0&0&0&0&0&0\\
1&1&0&1&0&1&1&1&1&0&0&0&0&0&0\\
1&1&1&0&1&1&1&1&1&0&0&0&0&0&0\\
1&1&0&1&0&1&1&1&1&0&0&0&0&0&0\\
0&0&1&1&1&0&1&0&0&1&1&0&0&0&0\\
0&0&1&1&1&1&0&1&0&1&1&1&1&1&0\\
0&0&1&1&1&0&1&0&1&1&1&1&1&1&0\\
0&0&1&1&1&0&0&1&0&0&0&1&1&1&0\\
0&0&0&0&0&1&1&1&0&0&1&0&0&0&0\\
0&0&0&0&0&1&1&1&0&1&0&1&0&0&1\\
0&0&0&0&0&0&1&1&1&0&1&0&1&0&1\\
0&0&0&0&0&0&1&1&1&0&0&1&0&1&1\\
0&0&0&0&0&0&1&1&1&0&0&0&1&0&0\\
0&0&0&0&0&0&0&0&0&0&1&1&1&0&0
\end{bmatrix} \qquad (2)$$

In the next phase, all anchors is clustered using compiled matrix RV. Criterion on which anchors are clustered is relatively simple. The first cluster is always consists in two known anchors, which is given in according to problem statement. Anchors, which has reliable radio path to both anchors in first cluster, belong to second cluster. Each of the anchors of subsequent clusters must have reliable radio path to three anchors forming part of preceding cluster. The result of this phase of algorithm is clusterization matrix CM number of rows of which corresponds to number of clusters. Each row of this matrix consists in anchors IDs which can be found in corresponding cluster and zeros (for compiling matrix of right form).

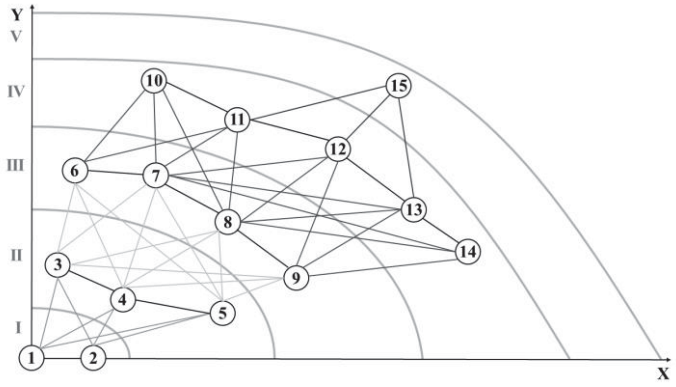

Fig.2. Example of anchors clusterization in according to proposed criterion

In Fig.2 an example of anchors clusterization in according to described criterion is presented.

For sake of clarity, the form of CM matrix for example in

$$CM = \begin{bmatrix} 1 & 2 & 0 & 0 & 0 & 0 & 0 & 0 & 0 & 0 & 0 & 0 & 0 & 0 \\ 1 & 2 & 3 & 4 & 5 & 0 & 0 & 0 & 0 & 0 & 0 & 0 & 0 & 0 \\ 1 & 2 & 3 & 4 & 5 & 6 & 7 & 8 & 9 & 0 & 0 & 0 & 0 & 0 \\ 1 & 2 & 3 & 4 & 5 & 6 & 7 & 8 & 9 & 10 & 11 & 12 & 13 & 14 \\ 1 & 2 & 3 & 4 & 5 & 6 & 7 & 8 & 9 & 10 & 11 & 12 & 13 & 14 & 15 \end{bmatrix} \quad (3)$$

Fig.2 is as follows:

In the next phase of algorithm, we sequentially use Kalman filter algorithm [9] for each row in CM matrix. Thus, filter give estimates of coordinates for all anchors in current cluster, which could be found in according to CM matrix.

Let's assume that there are N_{AtF} new anchors can be found in l-th cluster. Then, the state vector includes $2N_{AtF}$ elements and looks as follows:

$$\mathbf{x}_k = \begin{bmatrix} x_{j_k} \\ y_{j_k} \\ \vdots \\ x_{m_k} \\ y_{m_k} \end{bmatrix}, \quad (4)$$

where x_{j_k}, y_{j_k}, x_{m_k} and y_{m_k} – j-th and m-th anchor coordinates respectively.

Anchors coordinates dependences on time are considered as Wiener processes. Thus, the system dynamics is described by the following equations:

$$\begin{cases} x_{j_k} = x_{j_{k-1}} + \xi_k T \\ y_{j_k} = y_{j_{k-1}} + \xi_k T \\ \vdots \\ x_{m_k} = x_{m_{k-1}} + \xi_k T \\ y_{m_k} = y_{m_{k-1}} + \xi_k T \end{cases}. \quad (5)$$

In vector-matrix form, the above equations look like the following:

$$\mathbf{x}_k = F\mathbf{x}_{k-1} + G\xi_k, \quad (6)$$

where ξ_k – process noise of with zero mean and variance σ_ξ^2. F is transition matrix (square matrix with ones on main diagonal and size of which is $2N_{AtF}$) and G is process noise matrix. These matrices are written as follows:

$$F = \begin{bmatrix} 1 & \cdots & 0 \\ \vdots & \ddots & \vdots \\ 0 & \cdots & 1 \end{bmatrix}, \quad (7)$$

$$G = \begin{bmatrix} T \\ \vdots \\ T \end{bmatrix}, \quad (8)$$

where T is time interval between two measurements (system operating rate).

Each iteration of the Kalman filter algorithm can be divided into two parts: the prediction stage (extrapolation) and correction of prediction stage (estimation). The first stage includes finding extrapolated estimates of the state vector and the filtering noise covariance matrix, which can be written as:

$$\tilde{\mathbf{x}}_k = F\hat{\mathbf{x}}_{k-1}, \quad (9)$$

$$\tilde{D}_k = F\hat{D}_{k-1}F^T + GD_\xi G^T, \quad (10)$$

where D_ξ – process noise variance.

In the second part of the Kalman filter algorithm iteration, the extrapolated estimates of the state vector and the covariance matrix of filtering noises are corrected taking into account the measurements taken at this time, which can be written as follows:

$$K_k = \tilde{D}_k H_k^T \left(H_k \tilde{D}_k H_k^T + D_n \right)^{-1}, \quad (11)$$

$$\hat{D}_k = \tilde{D}_k - K_k H_k \tilde{D}_k, \quad (12)$$

$$\hat{\mathbf{x}}_k = \tilde{\mathbf{x}}_k + K_k S_k, \quad (13)$$

where K_k – filter weight coefficients matrix, S_k – the discrepancy between observations and extrapolated measurements, H_k – observation matrix and D_n – measurement noise covariance matrix.

The matrices S_k, H_k have the following form:

$$S_k = \tilde{r} - \begin{bmatrix} \sqrt{(\tilde{x}_{j_k} - x_{KA_v})^2 + (\tilde{y}_{j_k} - y_{KA_v})^2} \\ \vdots \\ \sqrt{(\tilde{x}_{j_k} - x_{KA_p})^2 + (\tilde{y}_{j_k} - y_{KA_p})^2} \\ \vdots \\ \sqrt{(\tilde{x}_{m_k} - x_{KA_u})^2 + (\tilde{y}_{m_k} - y_{KA_u})^2} \\ \vdots \\ \sqrt{(\tilde{x}_{m_k} - x_{KA_b})^2 + (\tilde{y}_{m_k} - y_{KA_b})^2} \\ \sqrt{(\tilde{x}_{j_k} - x_{q_k})^2 + (\tilde{y}_{j_k} - y_{q_k})^2} \\ \vdots \\ \sqrt{(\tilde{x}_{m_k} - x_{f_k})^2 + (\tilde{y}_{m_k} - y_{f_k})^2} \end{bmatrix} = \begin{bmatrix} \tilde{r}_{j\_KA_v} \\ \vdots \\ \tilde{r}_{j\_KA_p} \\ \vdots \\ \tilde{r}_{m\_KA_u} \\ \vdots \\ \tilde{r}_{m\_KA_b} \\ \tilde{r}_{j\_q} \\ \vdots \\ \tilde{r}_{m\_f} \end{bmatrix} - \begin{bmatrix} \sqrt{(\tilde{x}_{j_k} - x_{KA_v})^2 + (\tilde{y}_{j_k} - y_{KA_v})^2} \\ \vdots \\ \sqrt{(\tilde{x}_{j_k} - x_{KA_p})^2 + (\tilde{y}_{j_k} - y_{KA_p})^2} \\ \vdots \\ \sqrt{(\tilde{x}_{m_k} - x_{KA_u})^2 + (\tilde{y}_{m_k} - y_{KA_u})^2} \\ \vdots \\ \sqrt{(\tilde{x}_{m_k} - x_{KA_b})^2 + (\tilde{y}_{m_k} - y_{KA_b})^2} \\ \sqrt{(\tilde{x}_{j_k} - x_{q_k})^2 + (\tilde{y}_{j_k} - y_{q_k})^2} \\ \vdots \\ \sqrt{(\tilde{x}_{m_k} - x_{f_k})^2 + (\tilde{y}_{m_k} - y_{f_k})^2} \end{bmatrix}, \quad (14)$$

$$H_k = \begin{bmatrix} \frac{(\tilde{x}_{j_k} - x_{KA_1})}{\sqrt{(\tilde{x}_{j_k} - x_{KA_1})^2 + (\tilde{y}_{j_k} - y_{KA_1})^2}} & \frac{(\tilde{y}_{j_k} - y_{KA_1})}{\sqrt{(\tilde{x}_{j_k} - x_{KA_1})^2 + (\tilde{y}_{j_k} - y_{KA_1})^2}} & 0 & \dots & \dots & \dots & \dots & \dots & \dots & 0 \\ \vdots & \vdots & \vdots & \vdots & \vdots & \vdots & \vdots & \vdots & \vdots & \vdots \\ 0 & \dots & \frac{(\tilde{x}_{j_k} - x_{KA_e})}{\sqrt{(\tilde{x}_{j_k} - x_{KA_e})^2 + (\tilde{y}_{j_k} - y_{KA_e})^2}} & \frac{(\tilde{y}_{j_k} - y_{KA_e})}{\sqrt{(\tilde{x}_{j_k} - x_{KA_e})^2 + (\tilde{y}_{j_k} - y_{KA_e})^2}} & 0 & \dots & \dots & \dots & \dots & 0 \\ \vdots & \vdots & \vdots & \vdots & \vdots & \vdots & \vdots & \vdots & \vdots & \vdots \\ 0 & \dots & \dots & 0 & \frac{(\tilde{x}_{m_k} - x_{KA_1})}{\sqrt{(\tilde{x}_{m_k} - x_{KA_1})^2 + (\tilde{y}_{m_k} - y_{KA_1})^2}} & \frac{(\tilde{y}_{m_k} - y_{KA_1})}{\sqrt{(\tilde{x}_{m_k} - x_{KA_1})^2 + (\tilde{y}_{m_k} - y_{KA_1})^2}} & 0 & \dots & \dots & 0 \\ \vdots & \vdots & \vdots & \vdots & \vdots & \vdots & \vdots & \vdots & \vdots & \vdots \\ 0 & \dots & \dots & \dots & \dots & 0 & \frac{(\tilde{x}_{m_k} - x_{KA_e})}{\sqrt{(\tilde{x}_{m_k} - x_{KA_e})^2 + (\tilde{y}_{m_k} - y_{KA_e})^2}} & \frac{(\tilde{y}_{m_k} - x_{KA_e})}{\sqrt{(\tilde{x}_{m_k} - x_{KA_e})^2 + (\tilde{y}_{m_k} - y_{KA_e})^2}} & \dots & 0 \\ 0 & \dots & 0 & \frac{(\tilde{x}_{j_k} - x_{q_k})}{\sqrt{(\tilde{x}_{j_k} - x_{q_k})^2 + (\tilde{y}_{j_k} - y_{q_k})^2}} & \frac{(\tilde{y}_{j_k} - y_{q_k})}{\sqrt{(\tilde{x}_{j_k} - x_{q_k})^2 + (\tilde{y}_{j_k} - y_{q_k})^2}} & \dots & \frac{-(\tilde{x}_{j_k} - x_{q_k})}{\sqrt{(\tilde{x}_{j_k} - x_{q_k})^2 + (\tilde{y}_{j_k} - y_{q_k})^2}} & \frac{-(\tilde{y}_{j_k} - y_{q_k})}{\sqrt{(\tilde{x}_{j_k} - x_{q_k})^2 + (\tilde{y}_{j_k} - y_{q_k})^2}} & \dots & 0 \\ \vdots & \vdots & \vdots & \vdots & \vdots & \vdots & \vdots & \vdots & \vdots & \vdots \\ 0 & \dots & 0 & \frac{(\tilde{x}_{m_k} - x_{f_k})}{\sqrt{(\tilde{x}_{m_k} - x_{f_k})^2 + (\tilde{y}_{m_k} - y_{f_k})^2}} & \frac{(\tilde{y}_{m_k} - y_{f_k})}{\sqrt{(\tilde{x}_{m_k} - x_{f_k})^2 + (\tilde{y}_{m_k} - y_{f_k})^2}} & \dots & \frac{-(\tilde{x}_{m_k} - x_{f_k})}{\sqrt{(\tilde{x}_{m_k} - x_{f_k})^2 + (\tilde{y}_{m_k} - y_{f_k})^2}} & \frac{-(\tilde{y}_{m_k} - y_{f_k})}{\sqrt{(\tilde{x}_{m_k} - x_{f_k})^2 + (\tilde{y}_{m_k} - y_{f_k})^2}} & \dots & 0 \end{bmatrix} \quad (15)$$

where $\tilde{r}_{w\_KA_e}$ - measured range between w-th anchor (coordinate of which we estimate in current cluster) and KA_e - e-th known anchor in this cluster, $\tilde{r}_{m\_f}$ -measured mutual distance between two anchors coordinates of which is estimated in current cluster.

Thus, in the end of this phase we have estimates of all anchors which can be found in this cluster. After this step the set of discrepancies (14) stored on process of operating is checked. If discrepancies of any anchors exceed specified threshold, then calculations for this cluster repeated but with two distinctions: 1) anchors discrepancies of which don't exceed specified threshold became known for current cluster,

2) initial values for coordinates estimates of anchors which discrepancies exceed threshold are set in other quadrant of local coordinate system.

After this procedure we obtain coordinates of all deployed anchors which has enough amount reliable radio paths to other anchors.

IV. MODELLING

To investigate feasibility of proposed approach we carried out simulation modeling. We run 300 simulations and in each of them we randomly placed 15 anchors on area 50x50m and found coordinate estimates of 13 anchors with two given ones.

Parameters of modeling were the following:

Process noise standard deviation $\sigma_Q = 0.005$ m\s

Measurement noise standard deviation $\sigma_n = 0.1$ m.

Differences between true and estimated anchor coordinate in each simulation were stored and histogram shown below was plotted based on them.

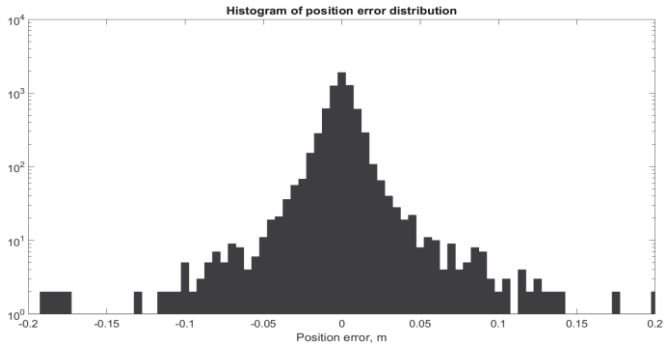

Fig.3. Histogram of total position error distribution

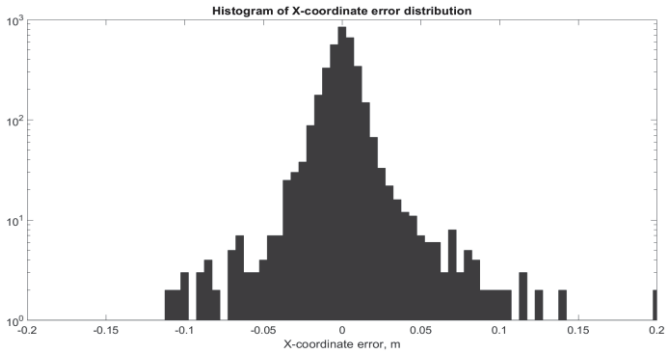

Fig.4. Histogram of X-coordinate position error distribution

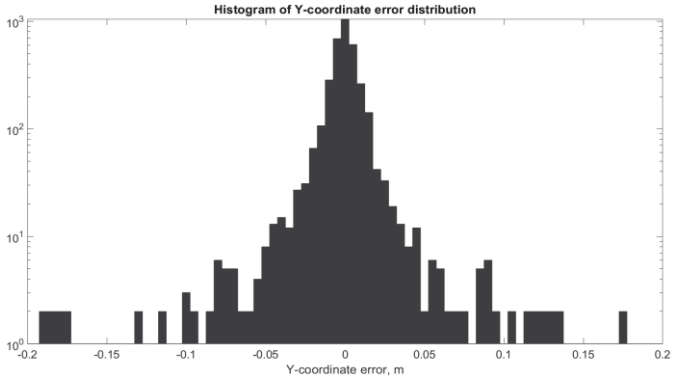

Fig.5. Histogram of Y-coordinate position error distribution

Main statistical characteristics (mean and standard deviation) of coordinate estimates of proposed algorithm based

on simulated data were found and consolidated into Table 1, presented below.

TABLE I. STATISTICAL CHARACTERISTICS OF COORDINATES ESTIMATES ERRORS OF PROPOSED ALGORITHM

Characteristic	Value, m
m_Σ	$-2.491 \cdot 10^{-4}$
σ_Σ	0.0242
m_x	$2.284 \cdot 10^{-4}$
σ_x	0.0274
m_y	$-7.267 \cdot 10^{-4}$
σ_y	0.0206

V. CONCLUSION

The proposed algorithm confirmed its feasibility in simulation modeling. The mean of total position error amounted to approximately $2.5 \cdot 10^{-4}$ meters (absolute value) and standard deviation equal to 0.0242 meters for chosen parameters of modeling.

As the next step in future work in this area, it is planned to verify presented algorithm on real UWB-based IPS.

REFERENCES

[1] A. Perov, V. Kharisov, "GLONASS. Construction and functioning principles," Radiotekhnika, Moscow, 2010.

[2] S. Wang, Y. Kobayashi, A.A. Ravankar, A. Ravankar, and T. Emaru, "A Novel Approach for Lidar-Based Robot Localization in a Scale-Drifted Map Constructed Using Monocular SLAM", *Sensors*, 2019.

[3] J. Lim, S. Lee, G. Tewolde and J. Kwon, "Indoor localization and navigation for a mobile robot equipped with rotating ultrasonic sensors using a smartphone as the robot's brain," *2015 IEEE International Conference on Electro/Information Technology (EIT)*, Dekalb, IL, 2015, pp. 621-625.

[4] Z. Qingxin, W. Luping and Z. Shuaishuai, "Strap-down inertial navigation system applied in estimating the track of mobile robot based on multiple-sensor," *2013 25th Chinese Control and Decision Conference (CCDC)*, Guiyang, 2013, pp. 3215-3218.

[5] A. Mikov, A. Panyov, V. Kosyanchuk and I. Prikhodko, "Sensor Fusion For Land Vehicle Localization Using Inertial MEMS and Odometry," *2019 IEEE International Symposium on Inertial Sensors and Systems (INERTIAL)*, Naples, FL, USA, 2019, pp. 1-2.

[6] V. Pasku et al., "Magnetic Field-Based Positioning Systems," *in IEEE Communications Surveys & Tutorials*, vol. 19, no. 3, pp. 2003-2017, thirdquarter 2017.

[7] F. Zafari, A. Gkelias and K. K. Leung, "A Survey of Indoor Localization Systems and Technologies," in *IEEE Communications Surveys & Tutorials*, vol. 21, no. 3, pp. 2568-2599, thirdquarter 2019.

[8] A. Chugunov et al., "Integration of Local Ultrawideband ToA/AOA Phase Difference of Arrival System and Inertial Navigation Systems," 2020 27th Saint Petersburg International Conference on Integrated Navigation Systems (ICINS), Saint Petersburg, Russia, 2020, pp. 1-8, doi: 10.23919/ICINS43215.2020.9133989

[9] A. Perov, Statistical theory of radio engineering systems (Statisticheskaya teoriya radiotechnicheskich sistem), Radiotekhnika, Moscow, 2003.